

## Cooling Performance of ALIP according to the Air or Sodium Cooling Type

Huee-Youl Ye\*, Jung Yoon, Tae-Ho Lee

Korea Atomic Energy Reserch Institute, Fast Reactor Development Division, 111, Daedeok-Daero 989 Beon-Gil, Yuseong-Gu, Daejeon, Korea

\*Corresponding author: yehuee@kaeri.re.kr

### 1. Introduction

The Annular Linear Induction Pump(ALIP) circulates the liquid sodium of Intermediate Heat Transport System(IHTS). ALIP pumps the liquid sodium by Lorentz force produced by the interaction of induced current in the liquid metal and their associated magnetic field. Even though the efficiency of the ALIP is very low compared to conventional mechanical pumps, it is very useful due to the absence of moving parts, low noise and vibration level, simplicity of flow rate regulation and maintenance, and high temperature operation capability[1].

Problems in utilization of ALIP concern a countermeasure for elevation of internal temperature of the coil due to joule heating and how to increase magnetic flux density of Na channel gap [2]. The conventional ALIP usually used cooling methods by circulating the air or water. On the other hand, GE-Toshiba developed a double stator pump adopting the sodium-immersed self-cooled type, and it recovered the heat loss in sodium. Therefore, the station load factor of the plant could be reduced.

In this study, the cooling performance with cooling types of ALIP is analyzed. We developed thermal analysis models to evaluate the cooling performance of air or sodium cooling type of ALIP. The cooling performance is analyzed for operating parameters and evaluated with cooling type.

### 2. Methods and Results

Fig. 1 shows the outer stator coil assembly of the PGSFR IHTS ALIP. Liquid sodium at 335°C flows axially through the inner duct. Steel laminations(i.e. Tooth and Yoke) are located around the outside of the duct and are held in place and tensioned against the duct wall by the alignment and spring housing assemblies located at the outside edge of the lamination blocks. The housing assemblies are mounted to a frame that is in turn mounted to the casing of the pump. Inside the casing, a nitrogen gas is filled to prevent oxidation of the coil. Copper coils are located inside of the steel laminations and are used to conduct electrical current in order to create the required magnetic field. As a result of the current flow, the coils are significantly heated internally by electrical resistance in the coils.

We performed thermal analysis of ALIP to evaluate the cooling performance. If one considers the thermal analysis as 1-D simplified problem and induces the

analytical solution, the sensitivity of the key variables can be analyzed, and the approximative trend can be figured. We considered simplified 1-D thermal analysis model, since 3-D analysis takes a lot of time and cost. The 1-D thermal analysis model was validated by comparing with 3-D model.

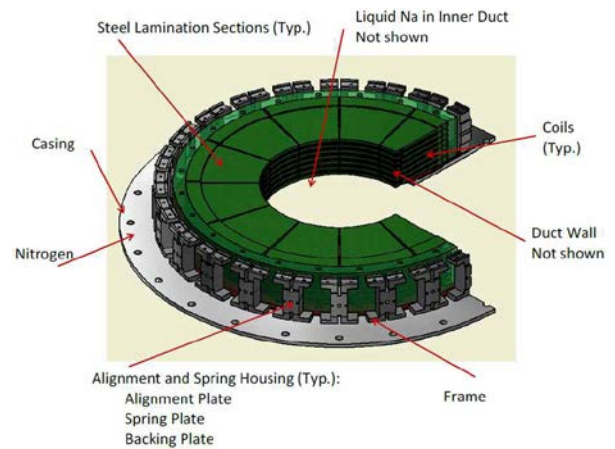


Fig. 1. Outer stator coil assembly.

#### 2.1 1-D Equivalent Thermal Analysis Model

The outer stator coil are simplified as shown in Fig. 2 for 1-D thermal analysis, and the thermal equivalent circuit for the simplified model is modeled as Fig. 3.

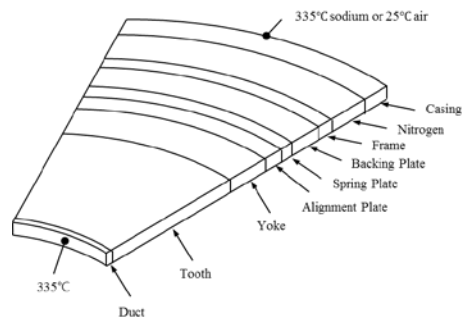


Fig. 2. Schematic diagram of the 1-D equivalent thermal model for ALIP.

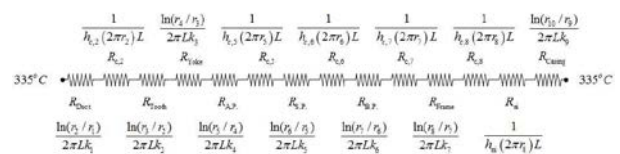


Fig. 3. Thermal equivalent circuit of ALIP.

The components of ALIP are modeled as simple blocks with an equivalent thermal conductivity and with contact thermal resistance between each part. Most of the heat generated in the coil is transmitted through the tooth, therefore, the coil and tooth can be simplified as a single block with equivalent heat generation per unit volume and equivalent thermal conductivity. The nitrogen region is assumed as infinite thermal conductivity, and contact thermal resistance between the casing and nitrogen is applied. The energy equation for the conductive heat transfer of each block is as follows.

$$\frac{1}{r} \frac{\partial}{\partial r} \left( r \frac{\partial T}{\partial r} \right) + \frac{\dot{q}_n}{k_n} = 0 \quad (1)$$

The boundary conditions of each block are as follows.

- Duct

$$\text{B.C.1: } T_1(0.25) = 335^\circ\text{C} \quad (2)$$

$$\text{B.C.2: } -k_1 \frac{\partial T_1}{\partial r} = h_{c,2} (T_1(0.255) - T_2(0.255)) \quad (3)$$

- Tooth

$$\text{B.C.3: } h_{c,2} (T_1(0.255) - T_2(0.255)) = -k_2 \frac{\partial T_2}{\partial r} \quad (4)$$

$$\text{B.C.4: } T_2(0.4464) = T_3(0.4464) \quad (5)$$

- Yoke

$$\text{B.C.5: } -k_2 \frac{\partial T_2}{\partial r} = -k_3 \frac{\partial T_3}{\partial r} \quad (6)$$

$$\text{B.C.6: } T_3(0.502) = T_4(0.502) \quad (7)$$

- Alignment Plate

$$\text{B.C.7: } -k_3 \frac{\partial T_3}{\partial r} = -k_4 \frac{\partial T_4}{\partial r} \quad (8)$$

$$\text{B.C.8: } -k_4 \frac{\partial T_4}{\partial r} = h_{c,5} (T_4(0.532) - T_5(0.532)) \quad (9)$$

- Spring Plate

$$\text{B.C.9: } h_{c,5} (T_4(0.532) - T_5(0.532)) = -k_5 \frac{\partial T_5}{\partial r} \quad (10)$$

$$\text{B.C.10: } -k_5 \frac{\partial T_5}{\partial r} = h_{c,6} (T_5(0.544) - T_6(0.544)) \quad (11)$$

- Backing Plate

$$\text{B.C.11: } h_{c,6} (T_5(0.544) - T_6(0.544)) = -k_6 \frac{\partial T_6}{\partial r} \quad (12)$$

$$\text{B.C.12: } -k_6 \frac{\partial T_6}{\partial r} = h_{c,7} (T_6(0.586) - T_7(0.586)) \quad (13)$$

- Frame

$$\text{B.C.13: } h_{c,7} (T_6(0.586) - T_7(0.586)) = -k_7 \frac{\partial T_7}{\partial r} \quad (14)$$

$$\text{B.C.14: } -k_7 \frac{\partial T_7}{\partial r} = h_{c,8} (T_7(0.596) - T_{ni}) \quad (15)$$

- Nitrogen

$$\text{B.C.15: } h_{c,8} (T_7(0.596) - T_{ni}) = h_{ni} (T_{ni} - T_8(0.676)) \quad (16)$$

- Casing

$$\text{B.C.16: } h_{ni} (T_{ni} - T_8(0.676)) = -k_8 \frac{\partial T_8}{\partial r} \quad (17)$$

$$\text{B.C.17: } T_8(0.706) = 335^\circ\text{C} \quad (18)$$

When the casing is cooled by the air, following boundary condition is used instead of the B.C. 17.

$$\text{B.C.17: } -k_8 \frac{\partial T_8}{\partial r} = h_a (T_8(0.706) - T_a) \quad (19)$$

Following correlations in accordance with Reynolds number range are applied for the heat transfer coefficient of Eq. (19).

$$Nu = \frac{h_a L}{k_a} = 0.664 \text{Re}_L^{0.5} \text{Pr}^{1/3}, \text{Re}_L < 5 \times 10^5 \quad (20)$$

$$Nu = \frac{h_a L}{k_a} = 0.037 \text{Re}_L^{0.8} \text{Pr}^{1/3}, 5 \times 10^5 \leq \text{Re}_L \leq 10^7 \quad (21)$$

Sixteen simultaneous equations with sixteen unknown variables can be generated by substituting above boundary conditions to Eq. (1). By solving the simultaneous equations, 1-D temperature profile of each part inside ALIP can be derived.

## 2.2 3-D Thermal Analysis Model

To validate the 1-D thermal analysis model, 3-D thermal analysis of ALIP has been performed. STAR-CCM+ Ver.9.02.007 is used for CFD analysis.

Since ALIP has symmetrical shapes with the axial and circumferential direction, 1/2 the coil and 1/2 the lamination block in the axial direction and the 30-degree lamination block in the circumferential direction is adopted. The analysis domain and mesh is shown at Fig. 4 and 5. The polyhedral mesh is used, and two prism layers are applied at near wall region to concentrate the lattice. The total number of mesh used in the analysis is 60,000. The assumptions and analysis method used for analysis are as follows.

- 3-D steady state: 1/12 circumferential symmetric
- Consideration of Conjugate Heat Transfer
- Turbulent model: Standard k- $\epsilon$  Two-Layer Model
- Two-Layer All y+ Wall Treatment
- Solver: Segregated Flow & Segregated Fluid Temperature

A symmetric plane condition is used for circumferential symmetry plane of the sodium, solid and air region, and other fluid surface used a no slip wall condition. 1/12 mass flow rate of IHTS normal operating condition is set for the inlet boundary condition of sodium, and pressure outlet condition is adopted for the outlet boundary. The velocity inlet and pressure outlet conditions are used for the air inlet and outlet boundaries respectively.

## 2.3 Validation

Fig. 6 shows the radial temperature distribution inside ALIP from 1-D and 3-D analysis models. It can be seen that 1-D equivalent thermal analysis model predicts well the temperature distribution within ALIP.

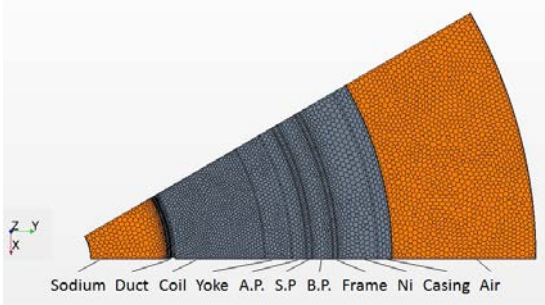


Fig. 4. Top view of the analysis domain.



Fig. 5. Side view of the analysis domain.

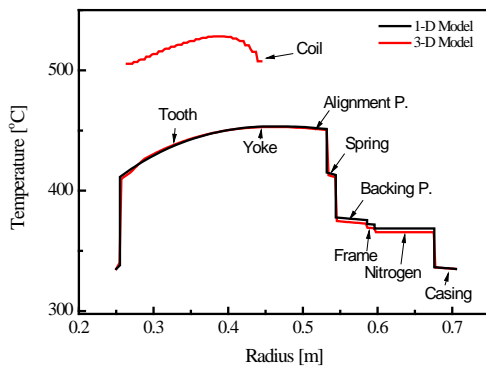


Fig. 6. Temperature distribution of ALIP from 1-D and 3-D model.

#### 2.4 Parameter Study

The temperature distribution inside ALIP is shown in Fig. 7, when the air velocity is set to 10, 5, 1, 0.2 and 0.1 m/s for air cooling type. The lower air velocity forms higher temperature distribution within the ALIP. The lower air velocity than 0.1 m/s forms higher temperature distribution than sodium cooling type. Therefore, the cooling performance for air cooling type is better than sodium cooling type at higher air velocity than 0.2 m/s.

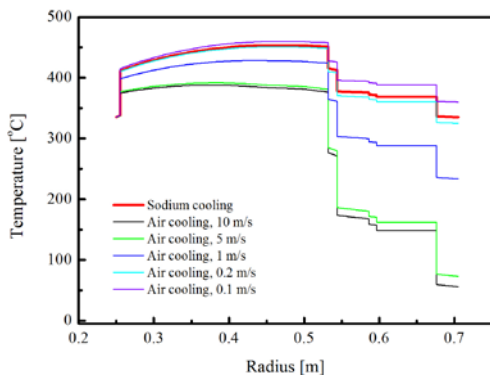


Fig. 7. Temperature distribution of ALIP for different air velocities.

Fig. 8 shows the temperature distribution for different air temperature with fixed air velocity of 1 m/s. The air temperature of below 270 °C can be confirmed that the air cooling performance is excellent as compared to sodium.

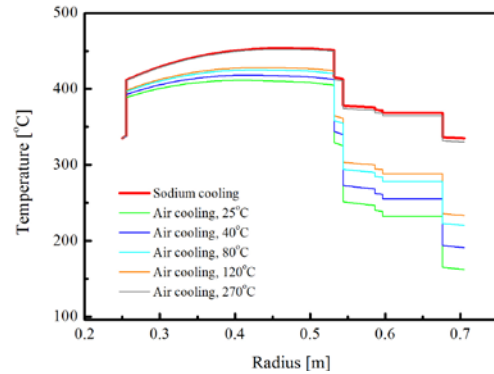


Fig. 8. Temperature distribution of ALIP for different air temperatures.

### 3. Conclusions

1-D and 3-D thermal analysis model for IHTS ALIP was developed, and the cooling performance was analyzed for air or sodium cooling type. The cooling performance for air cooling type was better than sodium cooling type at higher air velocity than 0.2 m/s. Also, the air temperature of below 270°C demonstrated the better cooling performance as compared to sodium. Therefore, in terms of cooling performance, it can be concluded that the air cooling type is much effective cooling method than sodium cooling type.

### ACKNOWLEDGEMENT

This work was supported by the National Research Foundation of Korea (NRF) grant funded by the Korea government (MSIP). (No. 2012M2A8A2025624).

### REFERENCES

- [1] N. Shamsuddeen, A. Ankit, J. Rajendrakumar, V. Krishna, and V. Jayashankar, Design and Analysis of Annular Linear Induction Pump (ALIP), Power System Technology and IEEE Power India Conference, p. 1-5, 2008.
- [2] H. Ota, K. Katsuke, M. Funato, J. Taguchi, A. W. Fanning, Y. Doi, N. Nibe, M. Ueta and T. Inagaki, Development of 160 m<sup>3</sup>/min Large Capacity Sodium-Immersed Self-Cooled Electromagnetic Pump, Journal of Nuclear Science and Technology, Vol. 41, p.511-523, 2004.